Mol. Cells *34*, 43-52, July 31, 2012
DOI/10.1007/s10059-012-0066-6
pISSN: 1016-8478 eISSN: 0219-1032

Molecules and Cells
http://molcells.org

Nicotiana tabacum Tsip1-Interacting Ferredoxin 1 Affects Biotic and Abiotic Stress Resistance

Sung Un Huh[1,3], In-Ju Lee[1], Byung-Kook Ham[2], and Kyung-Hee Paek[1,*]

Tsip1, a Zn finger protein that was isolated as a direct interactor with tobacco stress-induced 1 (Tsi1), plays an important role in both biotic and abiotic stress signaling. To further understand Tsip1 function, we searched for more Tsip1-interacting proteins by yeast two-hybrid screening using a tobacco cDNA library. Screening identified a new Tsip1-interacting protein, *Nicotiana tabacum* Tsip1-interacting ferredoxin 1 (NtTfd1), and binding specificity was confirmed both *in vitro* and *in vivo*. The four repeats of a cysteine-rich motif (CXXCXGXG) of Tsip1 proved important for binding to NtTfd1. Virus-induced gene silencing of *NtTfd1*, *Tsip1*, and *NtTfd1*/*Tsip1* rendered plants more susceptible to salinity stress compared with TRV2 control plants. *NtTfd1*- and *Tsip1*-silenced tobacco plants were more susceptible to infection by *Cucumber mosaic virus* compared with control plants. These results suggest that NtTfd1 might be involved in the regulation of biotic and abiotic stresses in chloroplasts by interaction with Tsip1.

INTRODUCTION

Tsip1 is a transcriptional co-activator of an EREBP/AP2-type transcription factor, Tsi1 (for Tobacco stress-induced gene 1), and relocalizes with Tsi1 to the nucleus from the chloroplast upon salicylic acid treatment (Ham et al., 2006; Park et al., 2001). The protein relocalization in response to biotic and abiotic stress signals are relatively common in plants (Caplan et al., 2008; Hwang and Sheen, 2001; Igarashi et al., 2001; Yeung et al., 2008) and could have evolved as a defense mechanism of plants to pathogens and environmental stresses. This could be an inefficient process because plants must expend much energy and time. *Tsip1* gene expression rapidly increases upon treatment with salicylic acid, ethephon, and salt, and upon exposure to pathogens (Ham et al., 2006). Dynamic gene expression patterns of Tsip1 suggest that Tsip1 alone or along with other binding-partner proteins can functionally respond to various extracellular signals.

Tsip1 has been identified as interacting with *Cucumber mosaic virus* (CMV) 1a protein using yeast two-hybrid screening (Huh et al., 2011). Tsip1 also interacts with CMV replicase complex protein, CMV 2a protein, in vacuolar membranes. Tsip1 might inhibit CMV replication by interacting with CMV replicase complex (Huh et al., 2011). These results indicate that Tsip1 specifically affects CMV infection by directly binding with the replication complex, although general heat-shock chaperone proteins facilitate replication of other RNA viruses (Banecki et al., 1996; Qiu et al., 2006).

Tsip1 contains a Zn-finger motif similar to the bacterial DnaJ-type protein and has been classified as a new DnaJ-type Zn finger protein (Ham et al., 2006). However, Tsip1 does not contain the DnaJ domain *per se* (Qiu et al., 2006). *In vitro*, Tsip1 does not exhibit chaperone activity (Huh et al., 2011). For example, N receptor-interacting protein 1 (NRIP1) for rhodanese sulfurtransferase normally localizes to the chloroplast but is relocalized from the chloroplast to the cytosolic region and nucleus by p50 effector protein of *Tobacco mosaic virus* (TMV). NRIP1 induces conformational change of tobacco N protein (Caplan et al., 2008). Thus, it may be inappropriate to classify Tsip1 as a DanJ-type chaperone protein, even though Tsip1 functions through physical interaction with Tsi1. Tsip1 might function as a conformational change-inducing component of target protein.

To carry out further functional study of Tsip1, Tsip1 as bait was used for yeast two-hybrid screening using the tobacco cDNA library. We found NtTfd1 as a Tsip1 binding partner and NtTfd1 directly interacted with Tsip1 in the chloroplast *in vitro* and *in vivo*. This interaction might confer enhanced biotic and abiotic stress tolerance *via* activation of diverse ferredoxin-associated pathways.

MATERIALS AND METHODS

Plant material and chemical treatments

Nicotiana tabacum cv. Samsun NN plants were grown in soil under a 16 h light and 8 h dark photoperiod. For gene expression analysis of *NtTfd1*, tobacco plants were treated with various chemicals and subjected to abiotic stresses. In some experiments, the plants were sprayed with 100 μM abscisic acid (ABA), 100 μM methyl viologen (MV), or 5 mM salicylic acid (SA) for various periods. In the case of salt (NaCl) and mannitol

[1]School of Life Sciences and Biotechnology, Korea University, Seoul 136-701, Korea, [2]Section of Plant Biology, College of Biological Sciences, University of California, California 95616, USA, [3]Present address: Jeju Biodiversity Research Institute, Jeju 699-943, Korea
*Correspondence: khpaek95@korea.ac.kr

Received March 2, 2012; accepted April 30, 2012; published online June 13, 2012

Keywords: *Cucumber mosaic virus*, *Nicotiana tabacum,* NtTfd1, Tsip1, VIGS

© The Korean Society for Molecular and Cellular Biology. All rights reserved.

treatments, the roots of tobacco plants were soaked in 300 mM NaCl, 400 mM mannitol or mock (distilled water, dH_2O).

To measure the chlorophyll contents, leaf discs from the *NtTfd1*-, *Tsip1*-, and *NtTfd1*/*Tsip1*-silenced plants were floated in 400 mM NaCl solution for 48 h. TRV2 leaf discs were used as a control. Chlorophyll contents (μg/g fresh weight) were measured at 48 h (Aono et al., 1993). The experiments were repeated two times with twelve leaf discs each time.

Yeast two-hybrid screening

The MatchMaker II GAL4 two-hybrid screening system (Clontech, USA) was used. The *Tsip1* cDNA fragment was cloned into pAS2-1 GAL4 binding domain (BD) expression vector. The pACT2 activation domain (AD) expression vector was used to make a cDNA library with the mRNA extracted from tobacco leaves. The two fusion vectors were co-transformed into *Saccharomyces cerevisiae* strain AH109 (*MATa, HIS3, lacZ, trp1, leu2,* and *ura3*). The transformed yeast cells were selected on minimal synthetic dropout (SD) medium lacking tryptophan, leucine, and histidine. Putative positive clones (Leu^+, Trp^+, and His^+) identified by colony-lift filter assay were selected by re-transformation. The plasmids were then transformed into *Escherichia coli* XL1-Blue cells (Stratagene, USA) by electroporation. The bacterially propagated pACT2 fusion plasmid was isolated and analyzed.

Glutathione-S-transferase (GST) pulldown assay

The *NtTfd1* open reading frame (ORF) was cloned into pGEX-3X vector (Amersham, USA). The plasmid was transformed into *E. coli* strain BL21 (DE3). GST-fused NtTfd1 protein was induced by 0.1 mM isopropyl-β-D-thiogalactoside (IPTG) at 30°C for 3 h. The culture was harvested by centrifugation and resuspended in lysis buffer (50 mM Na_2HPO_4, pH7.4, 300 mM NaCl, 10% glycerol, 1% Triton X-100) with 5% β-mercaptoethanol. Sonication was performed by Vibracell sonifier (Sonics and Materials, USA) for 1 min. Bacterial lysates were then centrifuged and the supernatant was purified by affinity chromatography for glutathione-agarose beads (Sigma-Aldrich, USA). Proteins bound to beads were washed with phosphate buffered saline (PBS), pH 7.4, and eluted with PBS containing 5 mM reduced glutathione (GSH). *Tsip1* mutant constructs under the control of T7 promoter were used as templates in coupled *in vitro* transcription/translation reactions of the TNT wheat germ system (Promega, USA). Proteins were synthesized for 1 h with ^{35}S-methione (Amersham) as a radiolabel. Five micrograms of GST-NtTfd1 fusion protein were mixed with 10 μl of *in vitro* translation mixture containing radiolabeled Tsip1 protein. To this mixture 10 μl of glutathione-aga-rose beads and 65 μl of binding buffer (20 mM Tris-HCl, pH 7.6, 100 mM KCl, 2 mM $CaCl_2$, 5 mM dithiothreitol, 0.5% glycerol) were added. As a control, the Tsip1 protein was mixed with glutathione-agarose beads only and, in another control, Tsip1 protein was incubated with GST protein itself. Protein pellets were then suspended in sample loading buffer, boiled, and electrophoresed using 15% sodium dodecyl sulfate-polyacry-laide gel electrophoresis (SDS-PAGE). After electrophoresis the gel was dried, exposed, and read with a BAS-2500 phosphorimager (Fuji Photo Film).

Protein expression and far-Western blot analysis

To investigate the interaction of NtTfd1 and Tsip1 *in vitro*, *Tsip1ΔCT*, *Tsip1ΔC4-2*, *Tsip1ΔNT*, and *Tsip1ΔCR* fragments were obtained by polymerase chain reaction (PCR) using various synthetic oligonucleotide primers using *Pfu* DNA polymerase (Stratagene). All obtained products were subcloned into pAS2-1 (Clontech, USA) and pGEX-3X vector (Amersham). *NtTfd1* cDNA was cloned into pGADT7 (Clontech).

Radiolabeled NtTfd1 protein for far-Western blot analysis was synthesized with the TNT T7-coupled wheat germ system (Promega) using ^{35}S-methione (Amersham) as a radiolabel. After linearization of *NtTfd1* fragment with endonuclease, the fragment was used for *in vitro* translation. The plasmids containing *Tsip1ΔCT*, *Tsip1ΔC4-2*, *Tsip1ΔNT*, and *Tsip1ΔCR* in the GEX-3X vector were transformed into *E. coli* strain BL21 (DE3). Protein overexpression of all GST-fused clones was induced by 0.5 mM isopropyl-β-D-thiogalactoside (IPTG) at 30°C for 3 h. The culture was harvested by centrifugation and resuspended in lysis buffer (50 mM Na_2HPO_4, pH 7.4, 300 mM NaCl, 10% glycerol, 1% Triton X-100). Sonication was performed by Vibracell sonifier for 1 min. Proteins were separated by 12% SDS-PAGE and transferred onto nitrocellulose membranes. Membranes were washed three times at 4°C in AC buffer (20 mM Tris-HCl, pH 7.5, 100 mM NaCl, 2.5 mM $MgCl_2$, and 75 mM KCl) containing 5% skim milk and incubated for 2 h in the presence of radiolabeled NtTfd1 protein probe in the same mixture. To eliminate the probe, the membranes were washed three times at 4°C with AC buffer. Dried membranes were visualized by autoradiography.

Gene expression analysis

Quantitative reverse transcription (qRT)-PCR was performed with SYBR Green (KapaBiosystems). Three independent biological replicate cDNA samples were tested for each experiment. Relative mRNA levels for each transcript were determined by the comparative CT method (Applied Biosystems, USA) as previously described (Schmittgen and Livak, 2008). Expression data was normalized with endogenous *NtEF1-α* gene as an internal reference. The following primer sets were used: *NtEF1-α*F 5′-AGACCACCAAGTACTACTGCAC-3′ and *NtEF1-α*R 5′-CCACCAATCTTGTACACATCC-3′, *Tsip1*F 5′-GATCCTTTGTTGAACGCATGGAAAA-3′ and *Tsip1*R 5′-GGATCCTTCGAGATGGCACTTGACAG-3′, *NtTfd1*F 5′-CTCTCATTATTTCAAAAAACAC-3′ and *NtTfd1*R 5′-AAGCAAATCAAAGTCATTGACTTG-3′, *NtERD10C*F 5′-CTCATGCCCAAGAGGAACAT-3′ and *NtERD10C*R 5′-GCCCGTCCTCTCCTATTTCT-3′, *NtC7*F 5′-TGCTTTTCGCTTGTGTTTTG-3′ and *NtC7*R 5′-TCATATCCGCGTCTACCACA-3′.

Virus-induced gene silencing (VIGS)

For the silencing of *NtTfd1* and *Tsip1* in *Nicotiana benthamiana*, the VIGS system of *Tobacco rattle virus* (TRV) vector was used (Jeon et al., 2010; Ratcliff et al., 2001). The 3′ untranslated regions (UTRs) of *NtTfd1* and *Tsip1* were cloned into TRV2 vector. For agro-infiltration, these constructs were introduced into *Agrobacterium tumefaciens* GV3101 strain using the freeze-thaw method (Weigel and Glazebrook, 2002) and the colonies were resuspended in infiltration buffer (20 mM citric acid, 2% sucrose, and 100 μM acetosyringone, pH 5.2). Approximately 4-week old *N. benthamiana* plants were infiltrated with *Agrobacterium* cells transformed with TRV1 and TRV2::*NtTfd1* or TRV2::*Tsip1* in a 1:1.5 ratio. For double silencing of *NtTfd1* and *Tsip1*, TRV1, TRV2::*NtTfd1*, and TRV2::*Tsip1* in a 1:1.5:1.5 ratio were co-infiltrated in *N. benthamiana.*

RNA and DNA blot hybridization analysis

For RNA blot analysis, 15 μg of total RNA were electrophoresed in a 1% agarose gel that contained 6% formaldehyde in MOPS buffer. The RNA was transferred to a Nytran Plus membrane (Schleicher and Schuell) in 10× SSC buffer. The mem-

brane was prehybridized at 65°C for 2 h in Church buffer (1% bovine serum albumin (BSA), 0.25 M disodium phosphate, pH 7.2, 1 mM EDTA, pH 8.0, 7% SDS). Hybridization was done with radiolabeled full-length *NtTfd1* gene probes for 16 h at 65°C. After hybridization, the membrane was washed with wash 1 buffer (0.5% BSA, 1 mM EDTA, 40 mM $NaHPO_4$, pH 7.2, 5% SDS) at 65°C for 5 min twice, and twice with wash 2 solution (1 mM EDTA, 40 mM $NaHPO_4$, pH 7.2, 1% SDS) at room temperature for 10 min each wash. The membrane was dried, wrapped, exposed, and read with a BAS-2500 phosphorimager (Fuji Photo Film).

For DNA blot analysis, restriction endonucleases *Xba*I, *Hin*dIII, and *Eco*RI were used for digestion of 15 μg of tobacco genomic DNA. After phenol extraction, the DNA fragment was separated by 0.8% agarose gel electrophoresis in 1× TBE buffer. The genomic DNA size was estimated using λ*Hin*dIII marker as a molecular size standard. The restricted genomic DNA was transferred to Nytran Plus membrane (Schleicher and Schuell) and depurinated for 10 min by ultraviolet light, denatured in a denaturing solution (1.5 M NaCl, 0.5 M NaOH) for 45 min, and treated with a neutralization solution (1.5 M NaCl, 0.5 M Tris-Cl, pH 8.0) for 45 min. Conditions of the Nytran Plus membrane transfer, radioisotope hybridization, wash, and exposure were the same as described above for RNA blot hybridization.

Polyethylene glycol (PEG)-mediated protoplast transformation

The *NtTfd1* and *Tsip1* constructs were placed under the control of the 35S CMV virus promoter in a pUC vector. The *NtTfd1*::*green fluorescent protein* (GFP), *Tsip1*::*red fluorescent protein* (RFP) fusion constructs were generated by placing the coding regions of these cDNAs in frame to the N terminus of GFP and RFP. The fusion constructs were introduced into *Arabidopsis* protoplasts prepared from whole seedlings by the PEG-mediated transformation method (Jofuku et al., 1994).

Bimolecular fluorescence complementation (BiFC) assay

For *in vivo* interaction analysis with NtTfd1 and Tsip1, a previously described BiFC assay (Walter et al., 2004) was used. *NtTfd1* and *Tsip1* ORFs were cloned into *Bam*H1 and *Xho*I sites of pSPYNE-35S or pSPYCE-35S vector. The constructs were transformed into *A. tumefaciens* strain C58C1 carrying the pCH32 helper plasmid. Agro-infiltration was performed in 4-week-old *N. benthamiana* plants. After 3-4 days co-infiltration, the epidermal cell layers of tobacco leaves were scanned for yellow fluorescent protein (YFP) signal using a LSM 510 META confocal microscope (Carl Zeiss, Germany).

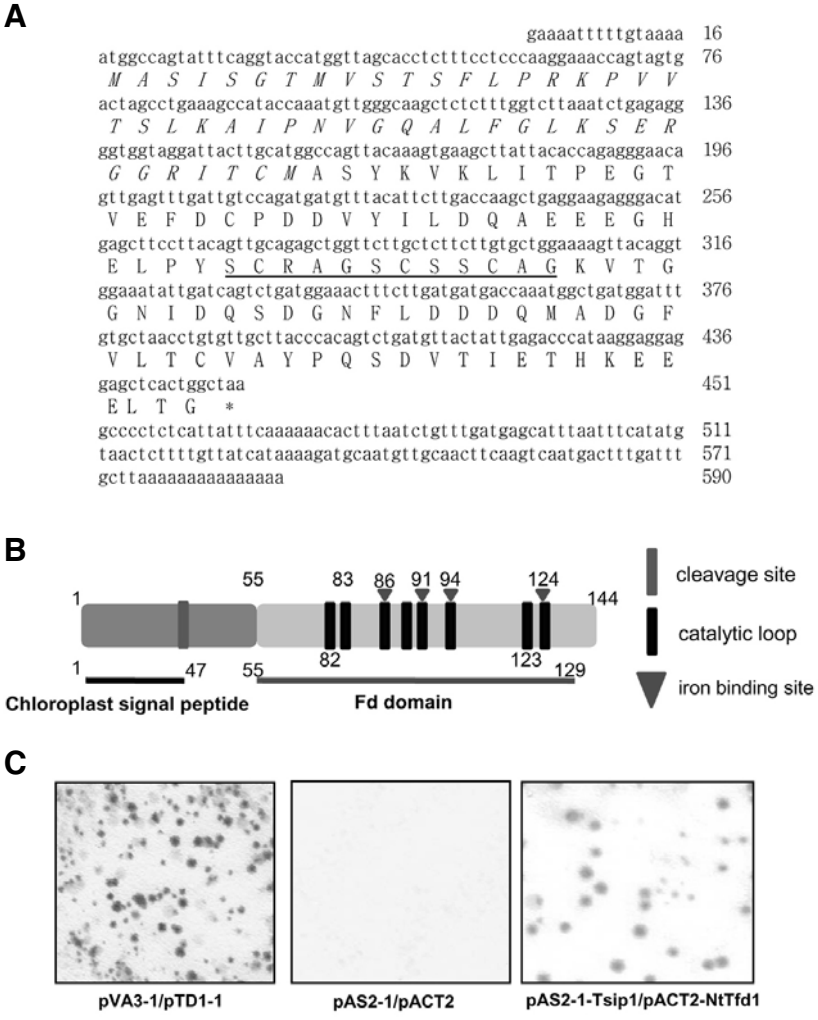

Fig. 1. Identification of tobacco ferredoxin 1 (NtTfd1) protein as a Tsip1-interacting protein. The nucleotide and the deduced amino acid sequence of the *NtTfd1* cDNA clone. The *NtTfd1* gene con-tained an open reading frame (ORF) of 435 bp encoding a poly-peptide of 145 amino acids. The chrolopast transit peptide is marked by italic letter and the iron-sulfer cluster domain of Fd, which plays a role in electron transfer, is underlined. (B) Schematic representation of NtTfd1 by bioinformatic tools. Chloroplast target signal peptide sequence and cleavage site were predicted by ChloroP1.1 server (http://www.cbs.dtu.dk/services/ChloroP/). Fd iron binding site and caltalytic loop were predicted by NCBI Conserved Domian Search (http://www.ncbi.nlm.nih.gov/Structure/cdd/wrpsb.cgi). (C) Activation of the GAL4 operon by the interaction between each designated bait and the putative interacting protein is shown by colony-lift filter assay. The spots indicate β-galactosidase activity on the X-gal substrate. The yeast strain Y187 containing the plasmids pVA3-1 and pTD1-1 were used as a positive control. pAS2-1 and pACT2 empty vectors in yeast cell were used as the negative control. The yeast strain Y187 containing the plasmids pAS2-1-Tsip1 and pACT2-NtTfd1 showed β-galactosidase activity in a colony-lift filter assay.

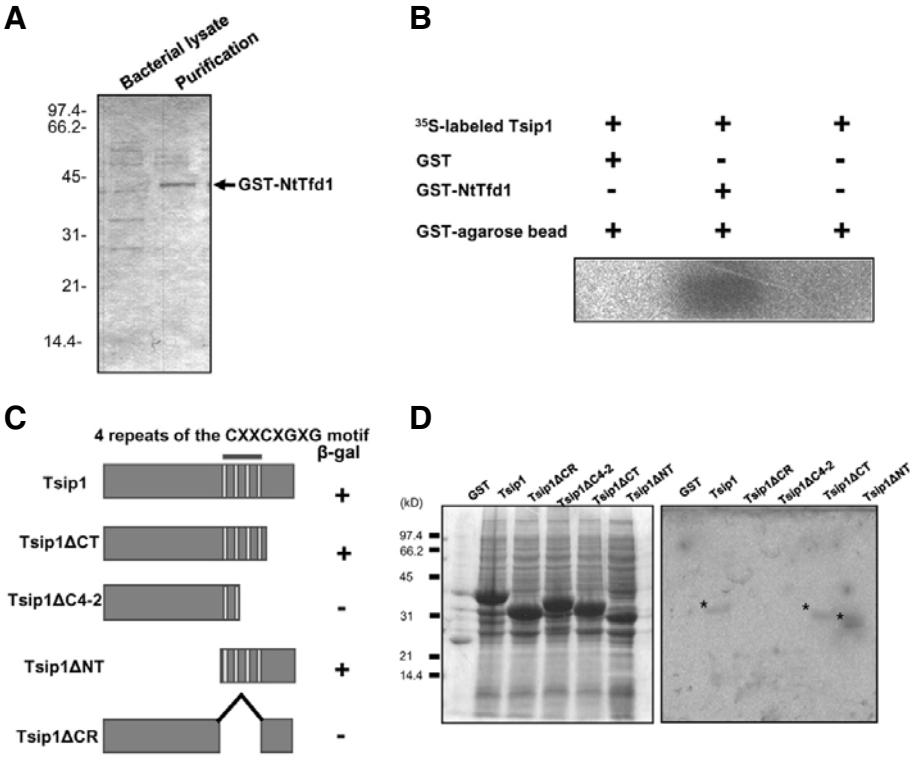

Fig. 2. Interaction of NtTfd1 with Tsip1 protein *in vitro*. (A) Affinity purification of GST-NtTfd1 fusion protein. The purified proteins were separated by 12% SDS-PAGE and stained with Coomassie brilliant blue. (B) *In vitro* binding assay. GST-NtTfd1 protein was incubated with *in vitro* translated ^{35}S-labeled Tsip1 protein and visualized by autoradiography. (C) Schematic representation of the constructs used in the yeast two-hybrid interation assay. The indicated regions of *Tsip1* were cloned into the bait vector pAS2-1 and the *Tsip1* bait plasmids were transformed with *NtTfd1* into the yeast. β-galactosidase activities are shown from the combination of individual *Tsip1* deletion constructs with *NtTfd1*. The symbol (+) indicates interaction and (-) indicates non-interaction. (D) *In vitro* binding assay results. Samples of GST-fused Tsip1 and Tsip1 deletion mutants were fractionated into insoluble fractions. Proteins were separated by 12% SDS-PAGE and stained with Comassie brilliant blue (left) or a far-Western blot analysis was performed to test binding of ^{35}S-labeled NtTfd1 probe to the immobilized Tsip1 deletion mutants (right). Asterisks indicate the binding.

In planta detection of hydrogen peroxide (H_2O_2)

Silenced plant leaves were excised and reactive oxygen species (ROS) production was detected by 3, 3-diaminobenzidine (DAB) staining (Orozco-Cardenas and Ryan, 1999).

RESULTS

Isolation of NtTfd1 as a Tsip1-interacting protein by yeast two-hybrid screening

Tsip1 was identified as a transcriptional co-activator by interaction with EREBP/AP2-type transcription factor Tsi1 (Ham et al., 2006; Park et al., 2001). To carry out further functional study of Tsip1, we performed yeast two-hybrid screening of tobacco cDNA library using Tsip1 as bait. Initially, 392 colonies were obtained from 1×10^6 cells on the Leu$^-$ and His$^-$ medium. The putative positive colonies were retransformed and subjected to the colony-lift filter assay to confirm β-galactosidase activities. The confirmed 26 colonies were classified as summarized in Supplementary Table S1. One was found most frequently as Tsip1-interactor. Sequence analysis of the clone revealed that the *NtTfd1* gene was 451 bp and the ORF encoded a putative protein of 145 amino acids with chloroplast transit peptide of 47 amino acids (Figs. 1A and 1B). We confirmed direct interaction between NtTfd1 and Tsip1 in the yeast two-hybrid system. pVA3-1 and pTD1-1 were used as positive controls exhibiting strong β-galactosidase activity, whereas empty vector used as a negative control did not show β-galactosidase activity (Fig. 1C). Co-transformants of *NtTfd1* fused to DNA BD and *Tsip1* fused to AD constructs were grown on selection medium. They exhibited strong β-galactosidase activity by the colony-lift filter assay (Fig. 1C). These results indicated that NtTfd1 was a Tsip1-interacting partner and that Tsip1 might regulate NtTfd1 in the chloroplast by a protein-protein interaction.

Plant chloroplasts have ferredoxins (Fds) that participate in electron flow in the chloroplast by receiving and donating electrons (Fukuyama, 2004; Hanke et al., 2004). Identified NtTfd1 also contained a putative single iron-sulfur cluster (Fe_2S_2) domain and catalytic loops that are conserved among all Fd proteins (Fig. 1B) (Fukuyama, 2004). This means that NtTfd1 could function as an electron carrier and could be instrumental for balancing electron cycle. To estimate *NtTfd1* gene copy numbers in the tobacco genome, DNA blot analysis was performed with *NtTfd1* full cDNA probe. As expected, tobacco plants displayed at least six copies of *NtTfd1* genes (Supplementary Fig. S1A). Next, we performed alignment of NtTfd1 with other plant Fds. As shown in Supplementary Figs. S2A and S2B, NtTfd1 showed the predicted evolutionary relationship with other Fds, being especially much closer with other tobacco Fd1 based on amino acid similarity. All the higher plant Fds were categorized into leaf-type and root-type. To determine the type of NtTfd1, we examined the organ-specific expression pattern of *NtTfd1* by RNA blot analysis. The *NtTfd1* gene expression levels were detected abundantly in the leaf, stem, and flower, whereas the transcripts were almost undetectable in root tissue (Supplementary Fig. S1B). These results indicated that NtTfd1 belongs to the evolutionarily conserved Fd and could be classified as leaf-type.

NtTfd1 interaction with Tsip1 *in vitro*

To determine the specific interaction between NtTfd1 and Tsip1, a GST-pull down assay was performed. GST-fused NtTfd1 was purified using a GST bead column. The purified GST-NtTfd1

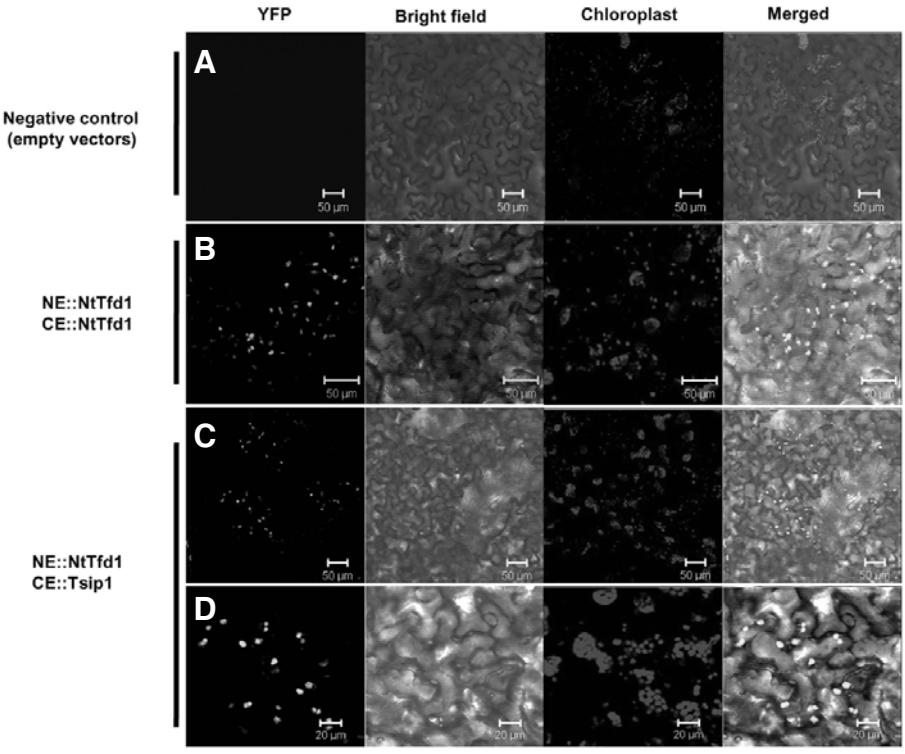

Fig. 3. *In vivo* interaction confirmation of NtTfd1 and Tsip1 in *N. benthamiana* by bimolecular fluorescence complementation (BiFC) assay. (A) Empty vector combination of pSPYNE-35S and pSPYCE 35S was co-expressed in *N. benthamiana* as a negative control. (B) NtTfd1 proteins formed homodimer complex. Yellow fluorescent protein (YFP) signals from BiFC were detected in the chloroplasts when pSPYNE-NtTfd1 and pSPYCE-NtTfd1 combinations were co-expressed in *N. benthamiana*. (C) NtTfd1 interacts with Tsip1 in chloroplasts. BiFC signals were detected in the chloroplasts when pSPYNE-NtTfd1 and pSPYCE-Tsip1 were co-expressed in *N. benthamiana*. (D) Enlarged image of Fig. 3C. Scale bar is indicated in the bottom. Red signal is chloroplast autofluorescence. The BiFC YFP signal is superimposed with bright-field image and chloroplast (red signal).

fusion protein size was approximately 43 kDa (Fig. 2A). The GST-NtTfd1 protein was incubated with *in vitro* translated Tsip1 protein. The eluted GST-NtTfd1 fusion protein was trapped on GST beads and formed complexes with ^{35}S-labeled Tsip1 protein (Fig. 2B). By contrast, no significant interaction signal was detected when the NtTfd1 was incubated with GST control protein or GST beads only (Fig. 2B). These data indicate that NtTfd1 directly interacts with Tsip1 *in vitro*.

Tsip1 has a four-repeat, cysteine-rich (CXXCXGXG) region that is important to binding with Tsi1 (Ham et al., 2006). To further dissect the interaction between NtTfd1 and Tsip1, we used various deletion constructs of Tsip1. The various constructs were fused to the GAL4 activation domain (Fig. 2C). These constructs were co-transformed with GAL4 DNA binding domain-NtTfd1 and β-galactosidase activity was determined. As shown in Fig. 2C, Tsip1, Tsip1ΔCT, and Tsip1ΔNT exhibited β-galactosidase activity, whereas the cysteine-rich deletion constructs did not show. We further confirmed the requirement for the cysteine-rich region in the interaction by far-Western blot analysis. The full Tsip1 and four truncated forms were expressed as GST-fusion proteins and these proteins were incubated with ^{35}S-labeled NtTfd1 protein. The *in vitro* translated NtTfd1 bound to GST-Tsip1, GST-Tsip1ΔCT, and GST-Tsip1ΔNT, whereas no significant interaction was detected with the GST protein, GST-Tsip1ΔC4-2, or GST-Tsip1ΔCR (Fig. 2D). These results indicated an important role for the cysteine-rich region of Tsip1 in binding to NtTfd1 protein.

NtTfd1 interaction with Tsip1 *in vivo*

As NtTfd1 contains putative chloroplast targeting signal peptide, we expected similar localization with Tsip1 in the chloroplast. To determine the localization of NtTfd1 *in vivo*, a GFP-fused *NtTfd1* construct was expressed in *Arabidopsis* protoplast by a PEG-mediated transient expression system (Yoo et al., 2007). GFP-NtTfd1 was predominantly localized to the chloroplast because the signal predominantly merged with chloroplast autosignal (Supplementary Fig. S3B), whereas the control soluble modified GFP was distributed uniformly in the cytosol (Supplementary Fig. S3A). Furthermore, when *GFP-NtTfd1* and *RFP-Tsip1* constructs were co-transformed in *Arabidopsis* protoplasts RFP-Tsip1 signals were merged with GFP-NtTfd1 signals in the chloroplast (Supplementary Fig. S3C). This data indicated that NtTfd1 and Tsip1 normally colocalize to the chloroplast.

Based upon the results obtained from the *in vitro* binding and NtTfd1 subcellular localization, we tested the *in planta* interaction of NtTfd1 and Tsip1 with the BiFC technique in *N. benthamiana*. *NtTfd1* and *Tsip1* were fused to the N-terminal YFP fragment (YFP^N) and the C-terminal fragment (YFP^C), respectively. Unfused YFP^N and YFP^C empty vector were used as a negative control, which did not induce YFP signals (Fig. 3A). NtTfd1-YFP^N and NtTfd1-YFP^C constructs strongly expressed YFP signals in chloroplasts (Fig. 3B) indicating that NtTfd1 can form a homodimer in chloroplasts. When the combination of NtTfd1 and Tsip1 was expressed, strong YFP fluorescence signals were observed and merged with chloroplast autosignals (Figs. 3C and 3D). These results suggested that NtTfd1 can directly interact with Tsip1 in chloroplasts and that NtTfd1 preferentially forms a homo- or heterodimer with target proteins.

Transcript levels of *Tsip1*, but not *NtTfd1*, are increased by the abiotic stress treatments

Previously, some plant *Fds* mRNA changed by the abiotic stress. For example, the *Arabidopsis Fd* mRNA levels were decreased under the condition of iron deficiency. As well, genome-wide analysis of *Arabidopsis thaliana* transcription profil-

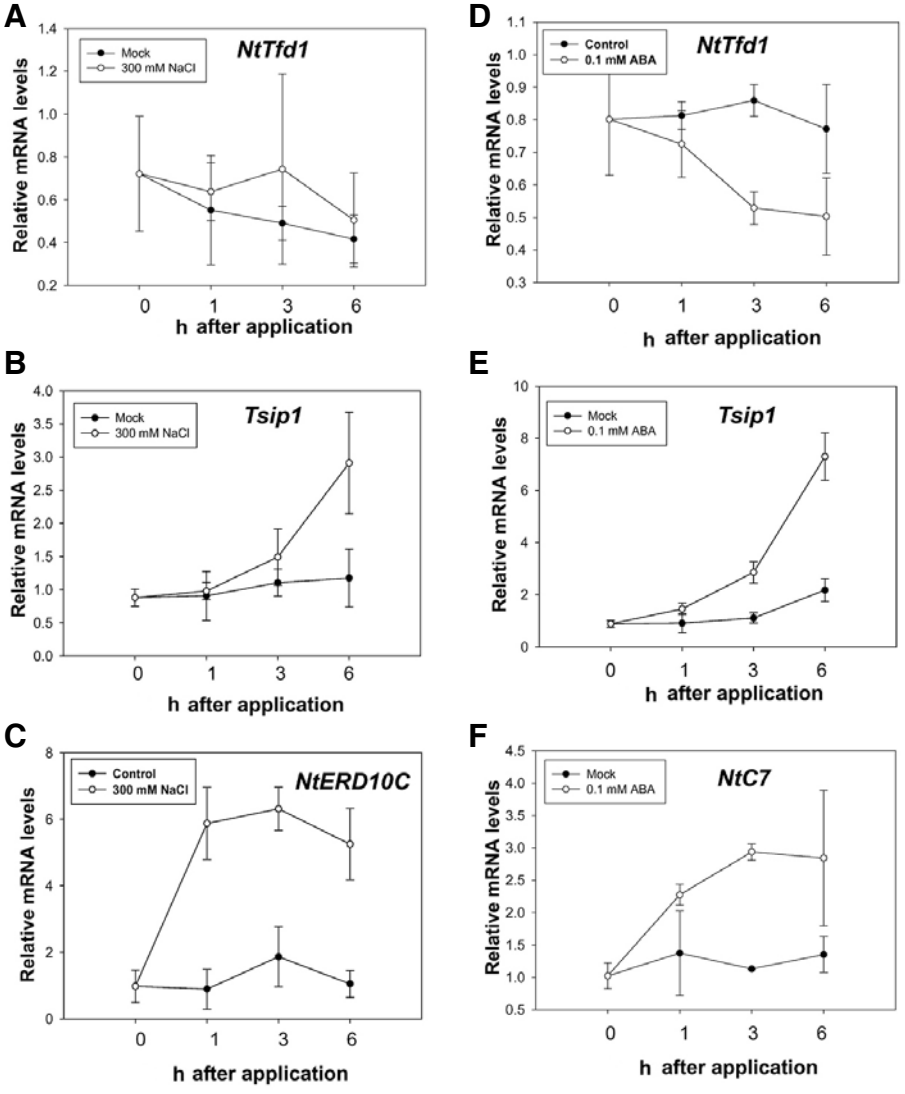

Fig. 4. Expression analysis of *NtTfd1* gene upon salt stress and exogenous ABA application. (A) Expression pattern of *NtTfd1* transcripts upon 300 mM NaCl treatment. (B) Expression pattern of *Tsip1* gene upon salt stress. (C) Expression pattern of *NtERD10C* as a positive control upon salt stress. (D) Expression pattern of *NtTfd1* transcripts upon exogenous 0.1 mM ABA application. (E) Expression pattern of *Tsip1* transcripts upon exogenous ABA application. (F) *NtC7* was used as a positive control upon ABA treatment. Expression data was normalized with an endogenous *NtEF1-α* gene. Error bars indicate standard deviation (n = 3).

ing exhibited consistently reduced levels of *Fd* mRNA during abiotic stress (Thimm et al., 2001; Zimmermann et al., 2004). Furthermore, the wheat leaf ferredoxin *PetF* mRNA levels are regulated by developmental change and light (Bringloe et al., 1995). To determine whether *NtTfd1* was associated with the abiotic stress response, *NtTfd1* and *Tsip1* expression pattern were monitored using qRT-PCR analysis of tobacco plants upon the NaCl, mannitol, and ABA treatments. Total RNA was extracted from the abiotic stressed tobacco plants leaves and mock-treated leaves at defined times. The *NtTfd1* transcript levels did not exhibit induced or reduced change under salt stress (Fig. 4A), but *Tsip1* mRNA levels are known to be increased by the same NaCl treatment condition (Ham et al., 2006) (Fig. 4B). *NtERD10C* was used as a positive control for the salt treatment (Wu et al., 2008) (Fig. 4C). In the mannitol stress condition, *NtTfd1* transcript levels were slightly up-regulated at 6 h, but did not significantly change (Supplementary Fig. S4A), while *Tsip1* mRNA levels were enhanced (Supplementary Fig. S4A). These results indicate that steady state levels of *NtTfd1* transcripts are not affected compared to control conditions, although enhanced *Tsip1* transcripts were detected with salt and mannitol abiotic stress treatments.

We also tested whether *NtTfd1* and *Tsip1* are involved in the ABA signaling pathway. Interestingly, expression levels of *NtTfd1* were significantly repressed upon ABA application (Fig. 4D). However, *Tsip1* transcript levels were up-regulated by ABA application (Fig. 4E). *NtC7* was used as a positive control for the ABA treatment (Tamura et al., 2003) (Fig. 4F). These results indicated the involvement of *NtTfd1* and *Tsip1* in the ABA-dependent pathway. On the other hand, we examined the transcript level of *NtTfd1* change upon exposure to SA as a defense-related plant hormone or MV as a ROS inducer. *NtTfd1* mRNA levels were not significantly changed by the SA and MV treatments, whereas *Tsip1* transcripts were increased in both treatment conditions (Supplementary Figs. S4B and S4C).

Silencing of *NtTfd1*, *Tsip1*, and *NtTfd1*/*Tsip1* increases salt stress sensitivity of tobacco plants

To further investigate the biological function of NtTfd1 and Tsip1, we performed a gene expression knockdown experiment using VIGS with each gene-specific cDNA fragments in *N. benthamiana* (Fig. 5A) (Burch-Smith et al., 2004). *NtTfd1*-silenced

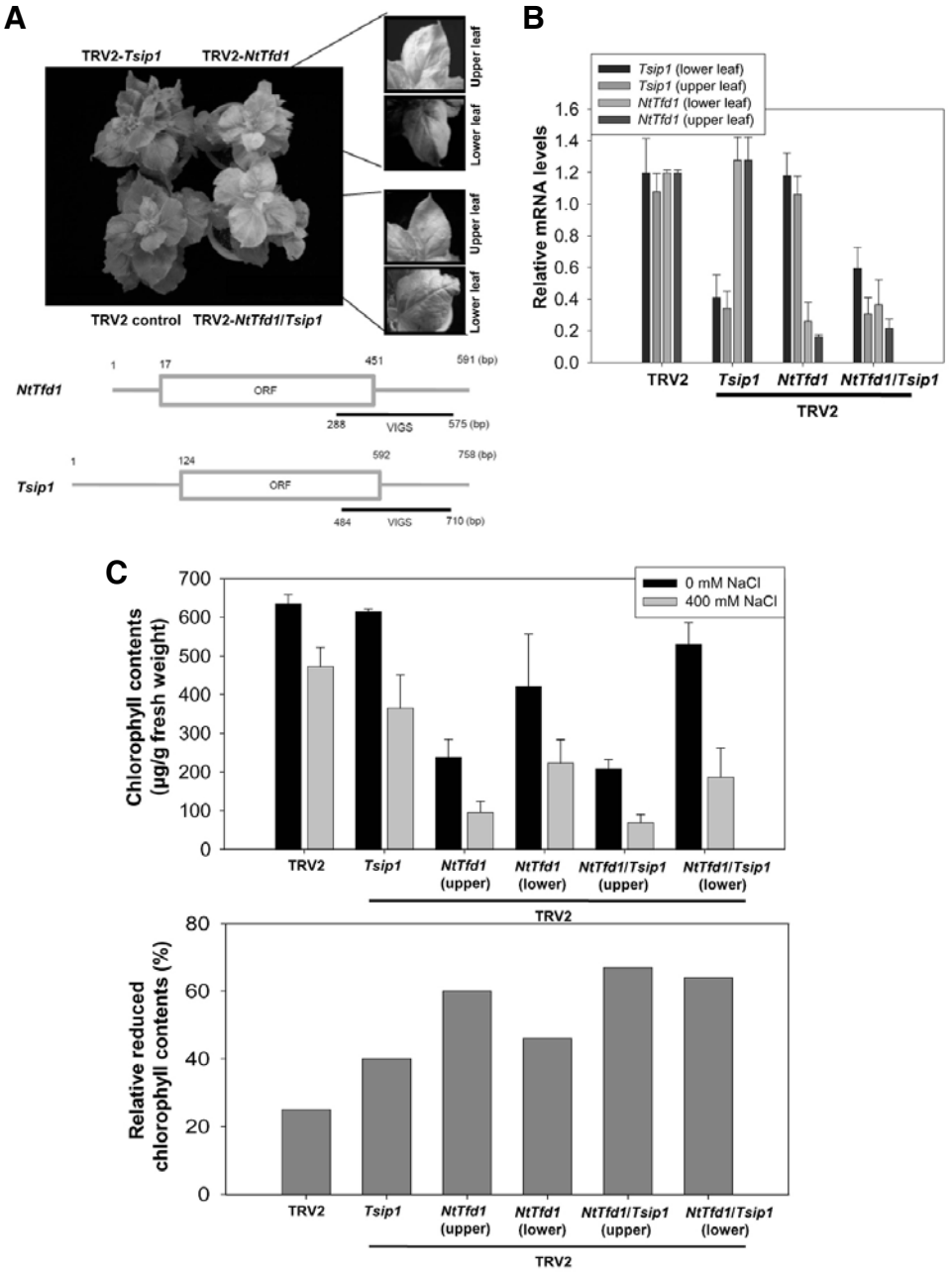

Fig. 5. Phenotype analysis of *NtTfd1* silencing and *NtTfd1*/*Tsip1* double silencing upon salt stress condition. (A) Silencing phenotype of TRV2::*NtTfd1*, TRV2::*Tsip1*, and TRV2::*NtTfd1*/*Tsip1*. Pale green phenotype was divided into upper (severe) and lower (mild) leaves. The bottom illustration shows VIGS region of *NtTfd1* and *Tsip1* for gene silencing. (B) Silencing levels of *NtTfd1* and *Tsip1* in the TRV2::*NtTfd1*, TRV2::*Tsip1*, and TRV2::*NtTfd1*/*Tsip1* plants upon salt stress (400 mM NaCl) condition. Error bars indicate strandard deviation (n = 5). (C) Chlorophyll contents and relative reduced chlorophyll contents of TRV2::*NtTfd1*, TRV2::*Tsip1*, and TRV2::*NtTfd1*/*Tsip1* plants upon 400 mM NaCl treatment. Error bars indicate standard deviation (n = 12).

plants had yellowish leaves (Fig. 5A) similar to antisense *Fed-1* transgenic plants of *N. benthamiana* (Ma et al., 2008). In upper leaves, *NtTfd1*-silenced plants showed strong yellowish phenotype, whereas a mild yellowish phenotype was evident in the lower leaves (Fig. 5A). To investigate the effects of salt stress in these silenced plants, gene expression of *NtTfd1* and *Tsip1* was checked upon salt treatment. *Tsip1* was induced in salt stress condition and the expression level of *NtTfd1* transcripts was reduced in *NtTfd1*-silenced plants (Fig. 5B). These results indicated that the yellowish phenotype reflects the efficiently silenced *NtTfd1* gene and is associated with inhibition of photosynthesis. *Tsip1*-silenced plants exhibited normal developmental phenotype compared with TRV2 control plants (Figs. 5A and 5B). However, *NtTfd1*/*Tsip1*-co-silenced plants showed a similar phenotype to *NtTfd1*-silenced plants (Figs. 5A and 5B).

To carry out functional analysis of *NtTfd1* and *Tsip1* upon abiotic stress, salt stress was chosen because Tsip1 is involved in salinity stress (Ham et al., 2006). In the presence of 400 mM NaCl, the chlorophyll content of *NtTfd1*-, *Tsip1*-, and *NtTfd1*/*Tsip1*-silenced plants were measured along with the control plants. We calculated the reduced chlorophyll ratio from *NtTfd1*-, *Tsip1*-, and *NtTfd1*/*Tsip1*-silenced plant leaf discs upon the 400 mM NaCl treatment compared with H_2O treatment. The reduced chlorophyll content ratios of *NtTfd1*/*Tsip1*-silenced plants more increased about 10% in upper leaves and 21% in lower leaves compared with *NtTfd1*-silenced plants (Fig. 5C). In addition, total chlorophyll content was decreased upon salt stress in the *Tsip1*-silenced plants without the yellowish leaf phenotype

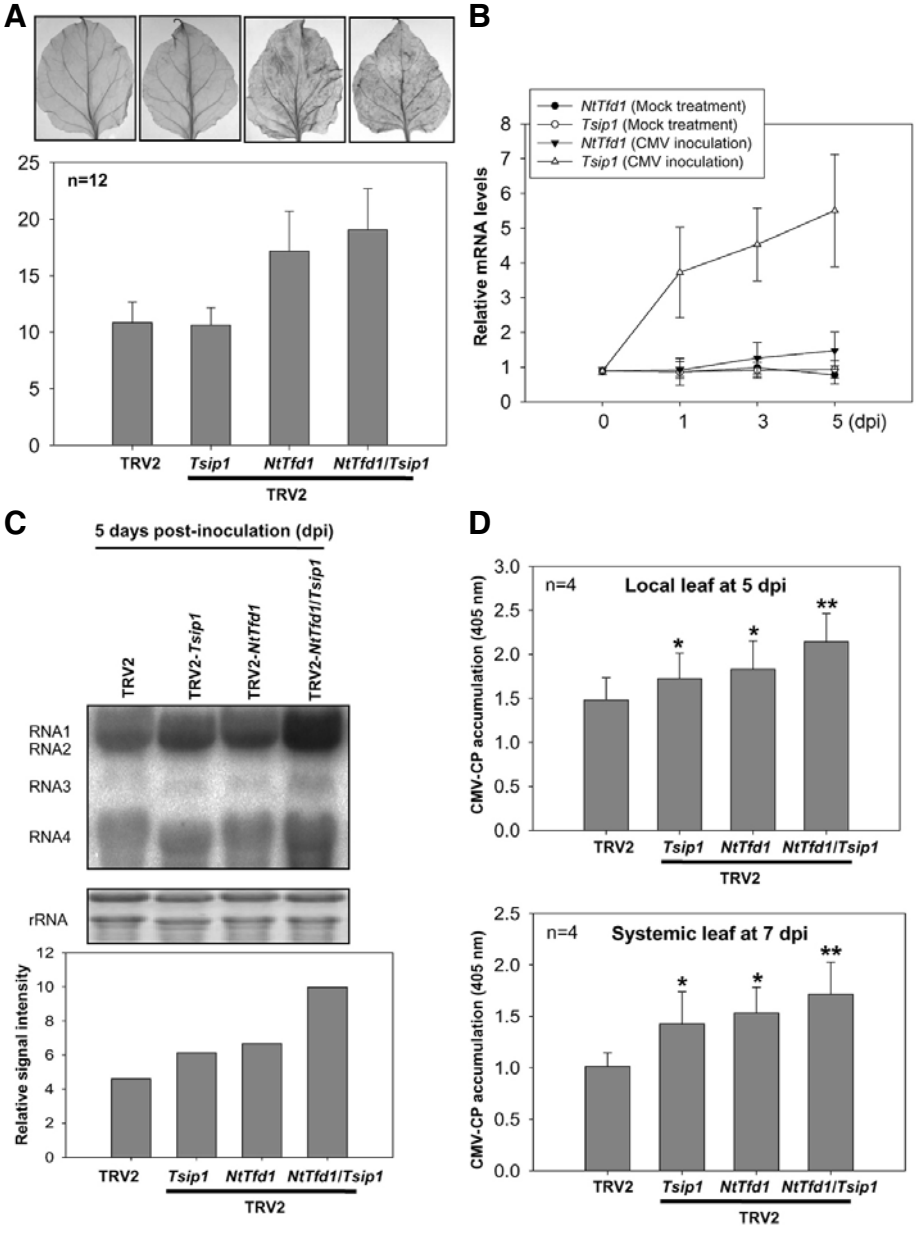

Fig. 6. Phenotype analysis of *NtTfd1* silencing and *NtTfd1*/*Tsip1* double silencing against CMV infection. (A) ROS detection in the TRV2 control, *Tsip1*-, *NtTfd1*-, and *NtTfd1*/*Tsip1*-silenced plants. Hydrogen peroxide was detected by DAB staining. Silenced plants were vacuum-infiltrated and incubated for 8 h. And then samples were further incubated in 70% ethanol until the chlorophyll was removed. DAB staining intensity was analyzed with image J program (http://rsbweb.nih.gov/ij/). Error bars indicate standard devia-tion (n = 12). (B) Expression pattern of *NtTfd1* and *Tsip1* upon CMV inoculation. CMV or mock inoculated plants were harvested and RNA samples were extracted by hot phenol method. Transcript levels were analyzed by quantitative RT-PCR. Error bars indicate standard deviation (n = 3). (C) RNA blot analysis in the TRV2 control, *Tsip1*-, *NtTfd1*-, and *NtTfd1*/*Tsip1*-silenced plants upon CMV inoculation. In CMV inoculated plants at 5 dpi, CMV RNAs were detected with CMV-3' UTR-specific probe. Signal intensity of RNA blot was analyzed with image J program. (D) CMV accumulation in both local (CMV inoculated) and systemic upper (non-inoculated) leaves was detected via indirect ELISA. Error bars indicate standard deviation (n = 4). Asterisks represent statistically significant differences between CMV inoculated TRV2 control and silenced plants (Student's *t*-test; $*p < 0.05$,$**p < 0.001$).

(Fig. 5C), suggesting that the *Tsip1*-silenced plants may still have less photosynthetic capacities than the wild-type without yellowish phenotype.

Silencing of *NtTfd1*, *Tsip1*, and *NtTfd1*/*Tsip1* leads to increased CMV susceptibility of tobacco plants

Fd overexpressing plants can be resistant to various pathogens mainly due to ROS production (Dayakar et al., 2003; Lin et al., 2010). However, in other reports, *Fd*-silenced tobacco plants exhibited enhanced ROS accumulation in normal condition and were more susceptible to biotic and abiotic stresses (Ma et al., 2008; Tognetti et al., 2006). To further analyze *NtTfd1* and *Tsip1* functions in biotic stress, we checked the endogenous ROS level in *NtTfd1*-, *Tsip1*-, and *NtTfd1*/*Tsip1*-silenced plants by DAB staining. *NtTfd1* and *NtTfd1*/*Tsip1*-silenced plants showed more accumulation of ROS compared with TRV2 and *Tsip1*-silenced plants (Fig. 6A).

Tsip1 transcripts are increased upon CMV infection and *Tsip1*is involved in defense response to CMV (Huh et al., 2011). Thus, we also checked *NtTfd1* expression upon CMV infection. *Tsip1* transcript levels were increased but *NtTfd1* did not show enhanced gene expression pattern upon CMV infection (Fig. 6B). Next, we inoculated CMV in *NtTfd1*- and *NtTfd1*/*Tsip1*-silenced plants to check ROS effect of CMV susceptibility. CMV RNAs accumulated slightly more in *NtTfd1*-silenced plants compared to *Tsip1*-silenced plants (Fig. 6C). Furthermore, *NtTfd1*/*Tsip1* double silenced plants accumulated more CMV RNAs compared with *Tsip1*- and *NtTfd1*-silenced plants (Fig. 6C). To confirm these CMV RNA level change phenotypes, an enzyme-linked immunosorbent assay was performed. In both local and systemic leaves, CMV-CP accumulation was increased in *Tsip1*-, *NtTfd1*-, and *NtTfd1*/*Tsip1*-silenced plants compared

with TRV2 control plants (Fig. 6D). Double silenced plants exhibited highly susceptible phenotypes compared with *Tsip1* and *NtTfd1* single silenced plants (Fig. 6D). These results demonstrated that, even though Tsip1 is not involved in ROS regulation, NtTfd1 is involved in ROS regulation. CMV infectivity seems to be affected in the plants by both ROS-dependent and ROS-independent manners.

DISCUSSION

NtTfd1 was presently identified as a Tsip1-interacting protein using a yeast two-hybrid system and its interaction with Tsip1 was demonstrated *in vitro* and *in vivo*. And the NtTfd1 and Tsip1 function is associated with biotic and abiotic stress. However, the function of NtTfd1 and Tsip1 interaction is not yet clear in chloroplasts, in terms of whether Tsip1 confers stability to the NtTfd1 protein with other protein interactions or affects NtTfd1 in a redox-independent mechanism.

Most higher plant chloroplasts have Fds that make electrons available in chloroplasts by receiving and donating electrons from photosystem I to NADPH, catalyzed by Fd:$NADP^+$ oxidoreductase. Reduced Fd reduces either thioredoxin *via* Fd:thioredoxin reductase or NADP via Fd:NADP reductase (Fukuyama, 2004; Hanke et al., 2004). Furthermore, reduced Fd donates the electrons to other metabolic pathways by interacting with various enzymes in the chloroplast (Knaff and Hirasawa, 1991; Kurisu et al., 2001) although Fd also functions in nonphotosynthetic cells like root tissues (Terauchi et al., 2009). These complex formations between Fds and Fd-dependent enzymes, such as nitrite and sulfite reductases, glutamine-oxoglutarate amidotransferase, and stearoyl-ACPΔ9-desaturase are important in diverse functions (Akashi et al., 1999; Fredricks and Stadtman, 1965; Nakamura and Nara, 2004).

Some Fds function in biotic stress *via* protein-protein interaction or modulation of defense response. For example, the chloroplast precursor of ferredoxin-5 from maize (*Zea mays*) directly interacts with the HC-Pro protein of Sugar cane mosaic virus *in vivo* (Cheng et al., 2008). The sweet pepper plant ferredoxin-like protein is involved in the harpin-mediated hypersensitive cell death via increased active oxygen species generation. Furthermore, overexpression of *Fds* exhibited enhanced tolerance to abiotic stresses. The bacterial *flavodoxin*-expressing transgenic tobacco plants exhibit enhanced tolerance to iron starvation and diverse stresses (Tognetti et al., 2006; 2007). Thus, it is possible that NtTfd1 function is unusually involved in independent oxidoreductive pathways and photosynthesis. These involvements also could play important roles in biotic and abiotic stress.

Subcellular localization of Tsip1 in chloroplasts is not only at the outer surface but also at the stroma (Ham et al., 2006). NtTfd1 also localizes to the chloroplast stroma and may be important to regulate redox state or other electron transfer. Presently, we demonstrated the interaction of NtTfd1 and Tsip1 in chloroplasts, especially in the stroma region. These results imply that Tsip1 normally interacts with NtTfd1 in the chloroplasts and this interaction might be associated with stability of protein-protein complex. Fd forms a non-covalent ternary complex, Fd:FTR:Trx-*m* (Xu et al., 2009). Unusually, maize Fd V protein was revealed as an interaction partner of a HC-Pro protein of SCMV and HC-Pro protein affected negatively the *Fd V* mRNA levels (Cheng et al., 2008). These results demonstrate that Fds might form a complex with other binding partner proteins and play a role in defense against attack from diverse pathogens.

ROS play an important role in plant defense against pathogens and environmental stress (Gill and Tuteja, 2010; Mittler et al., 2004), but evidence for their role in defense or tolerance is still not clear. In *NtTfd1*- and *NtTfd1*/*Tsip1*-silenced plants, we found highly accumulated ROS. However, the enhanced ROS increased the susceptibility of the plants to salinity stress and to CMV infection. *Tsip1*-silenced plants exhibited undetectable ROS levels compared with TRV2 control plants. These results suggest that susceptibility phenotype of *Tsip1*-silenced plants against CMV infection or salinity stress does not involve the ROS-defense system.

The inhibition of photosynthesis by pathogens might be a major strategy for infection and salinity stress also affects the photosynthesis pathway (Berger et al., 2007; Gill and Tuteja, 2010). We also found that Tsip1 has diverse putative interaction proteins of chloroplasts in yeast two-hybrid screening. These include proteins such as Rubisco small subunit, thiamin biosynthesis protein, and cytochrome B6-F complex subunit protein (Supplementary Table S1). *Tsip1*-overexpressed transgenic plants showed tolerance to salinity stress and resistance to CMV infection (Ham et al., 2006; Huh et al., 2011). Thus, it is possible that Tsip1 might confer stability of NtTfd1 and other proteins via protein-protein interaction in the chloroplasts.

Note: Supplementary information is available on the Molecules and Cells website (www.molcells.org).

ACKNOWLEDGMENTS

This work was supported by the Science Research Center-Engineering Research Center Program (Plant Signaling Network Research Center) of the Ministry of Education, Science and Technology (R11-2003-008-02001-0), the Mid-career Researcher-Program through a National Research Foundation grant funded by the Ministry of Education Science and Technology (MEST) (2009-0085565), and the Wujangchoon Project (PJ007850) from the Rural Development Administration, Republic of Korea.

REFERENCES

Akashi, T., Matsumura, T., Ideguchi, T., Iwakiri, K., Kawakatsu, T., Taniguchi, I., and Hase, T. (1999). Comparison of the electrostatic binding sites on the surface of ferredoxin for two ferredoxin-dependent enzymes, ferredoxin-NADP(+) reductase and sulfite reductase. J. Biol. Chem. *274*, 29399-405.

Aono, M., Kubo, A., Saji, H., Tanaka, K., and Kondo, N. (1993). Enhanced tolerance to photooxidative stress of transgenic *Nicotiana tabacum* with high chloroplastic glutathione reductase activity. Plant Cell Physiol. *34*, 129-135.

Caplan, J.L., Mamillapalli, P., Burch-Smith, T.M., Czymmek, K., and Dinesh-Kumar, S.P. (2008). Chloroplastic protein NRIP1 mediates innate immune receptor recognition of a viral effector. Cell *132*, 449-462.

Fukuyama, K. (2004). Structure and function of plant-type ferredoxins. Photosynth Res. *81*, 289-301.

Ham, B.K., Park, J.M., Lee, S.B., Kim, M.J., Lee, I.J., Kim, K.J., Kwon, C.S., and Paek, K.H. (2006). Tobacco Tsip1, a DnaJ-type Zn finger protein, is recruited to and potentiates Tsi1-mediated transcriptional activation. Plant Cell *18*, 2005-2020.

Hanke, G.T., Kimata-Ariga, Y., Taniguchi, I., and Hase, T. (2004). A post genomic characterization of Arabidopsis ferredoxins. Plant Physiol. *134*, 255-264.

Hwang, I., and Sheen, J. (2001). Two-component circuitry in Arabidopsis cytokinin signal transduction. Nature *413*, 383-389.

Igarashi, D., Ishida, S., Fukazawa, J., and Takahashi, Y. (2001). 14-3-3 proteins regulate intracellular localization of the bZIP transcriptional activator RSG. Plant Cell *13*, 2483-2497.

Jeon, Y., Hwang, A.R., Hwang, I., and Pai, H.S. (2010). Silencing of *NbCEP1* encoding a chloroplast envelope protein containing 15

leucine-rich-repeats disrupts chloroplast biogenesis in *Nicotiana benthamiana*. Mol. Cells *29*, 175-183.
Jofuku, K.D., den Boer, B.G., Van Montagu, M., and Okamuro, J.K. (1994). Control of Arabidopsis flower and seed development by the homeotic gene APETALA2. Plant Cell *6*, 1211-1225.
Park, J.M., Park, C.J., Lee, S.B., Ham, B.K., Shin, R., and Paek, K.H. (2001). Overexpression of the tobacco Tsi1 gene encoding an EREBP/AP2-type transcription factor enhances resistance against pathogen attack and osmotic stress in tobacco. Plant Cell *13*, 1035-1046.
Ratcliff, F., Martin-Hernandez, A.M., and Baulcombe, D.C. (2001). Technical Advance. Tobacco rattle virus as a vector for analysis of gene function by silencing. Plant J. *25*, 237-245.
Walter, M., Chaban, C., Schutze, K., Batistic, O., Weckermann, K., Nake, C., Blazevic, D., Grefen, C., Schumacher, K., Oecking, C., et al. (2004). Visualization of protein interactions in living plant cells using bimolecular fluorescence complementation. Plant J. *40*, 428-438.
Weigel, D., and Glazebrook, J. (2002). Arabidopsis: a laboratory manual (Cold Spring Harbor, N.Y.; Cold Spring Harbor Laboratory Press).
Yeung, T., Gilbert, G.E., Shi, J., Silvius, J., Kapus, A., and Grinstein, S. (2008). Membrane phosphatidylserine regulates surface charge and protein localization. Science *319*, 210-213.